GMR
The Original

SUSTAINABLE GREEN FABRICATION OF POLYMERIC ELECTROSPUN NANOSCAFFOLDS LOADED WITH CuO NANOPARTICLES FOR ANTICANCER ACTIVITY ON HT-29 AND MCF-7 CELLS

Pooja Yagavel[1], Gayathri Narayanan[2], Alagendran Subbarayalu[3]*

[1]Saveetha Medical College & Hospital (SMCH), Saveetha Institute of Medical and Technical Sciences (SIMATS), Thandalam, Chennai, Tamil Nadu 602105, India. poojayagavel92@gmail.com
[2]Department of Pathology, Saveetha Medical College and Hospital, Saveetha Institute of Medical And Technical Sciences (SIMATS), Thandalam, Chennai-602105, Tamil Nadu, India. Email: drgayathrinarayanan@gmail.com; ORCID: https://orcid.org/0009-0002-2686-6112.
[3]Clinical Neuroscience and Phytomedicine Laboratory, Department of Research, Saveetha College of Nursing (SCON), Saveetha Institute of Medical and Technical Sciences (SIMATS), Chennai 602105, Tamil Nadu, India. Email: proteinblg@gmail.com; alagendrans.scon@saveetha.com. ORCID: https://orcid.org/0009-0009-0749-7180.
*Correspondence: proteinblg@gmail.com; alagendrans.scon@saveetha.com (A.S.)

ABSTRACT
This study presents the green synthesis of copper oxide (CuO) nanoparticles using *Turbinaria ornata* extract and their integration into starch/polyvinyl alcohol (PVA)-based nanofibrous scaffolds for potential anticancer applications. UV–Visible spectroscopy confirmed nanoparticle formation through a sharp absorption band near 200 nm, while Fourier-transform infrared spectroscopy (FTIR) analysis revealed functional groups indicative of phytochemical capping and successful polymer embedding. X-ray diffraction (XRD) confirmed the monoclinic crystalline structure of CuO nanoparticles and their uniform dispersion within the polymer matrix. Scanning electron microscopy (SEM) showed spherical nanoparticles and smooth, bead-free nanofibers with homogeneous nanoparticle distribution. Thermogravimetric analysis (TGA) indicated enhanced thermal stability due to nanoparticle incorporation. Dynamic light scattering (DLS) and zeta potential analysis revealed a hydrodynamic diameter of 92.8 nm and moderate colloidal stability. Cytotoxicity assays demonstrated dose-dependent anticancer activity, with starch/PVA/CuO nanoscaffolds exhibiting the highest potency against HT-29 and MCF-7 cell lines. These findings highlight the potential of CuO-loaded nanofibers as effective biomaterials for cancer therapy.

KEYWORDS: *Turbinaria ornata*, Green synthesis, CuO nanoparticles, Starch/PVA nanoscaffolds, Anticancer activity.

1. INTRODUCTION

Cancer continues to pose a formidable challenge to global healthcare systems, ranking among the leading causes of mortality worldwide [1-3]. Despite the advent of targeted therapies and immunotherapies, conventional treatment modalities such as chemotherapy remain hampered by severe side effects, drug resistance, and non-specific cytotoxicity [4, 5]. This scenario has necessitated the exploration of alternative strategies that leverage biomaterials and nanotechnology to enhance therapeutic efficacy while minimizing systemic toxicity [6, 7]. In this regard, the development of biocompatible nanomaterials, particularly those engineered through green and sustainable approaches, offers a promising path toward more effective cancer treatment solutions [8].

Among various nanostructured materials, electrospun nanofibrous scaffolds have emerged as highly versatile platforms in biomedical applications, especially for drug delivery, wound healing, and tissue engineering [9, 10]. Their high surface area-to-volume ratio, tunable porosity, and morphological resemblance to the extracellular matrix (ECM) make them ideal candidates for controlled drug release and cell-interactive applications [11, 12]. Integrating nanoparticles into polymeric nanofibers further enhances their functionality, providing combined benefits of mechanical stability, bioactivity, and sustained therapeutic delivery [13, 14].

Copper oxide nanoparticles (CuO NPs) have garnered significant attention due to their exceptional antimicrobial, antioxidant, and anticancer properties [15, 16]. Owing to their cost-effectiveness, inherent redox potential, and the ability to generate reactive oxygen species (ROS), CuO NPs disrupt cancer cell proliferation and induce apoptosis via oxidative stress mechanisms [17-20]. However, conventional methods for CuO NP synthesis often involve toxic chemicals and high-energy processes, which may compromise the biocompatibility and

environmental safety of the final product [21]. As an alternative, green synthesis using plant or algal extracts has gained traction as a sustainable and eco-friendly route, offering natural reducing and stabilizing agents in the synthesis of metal oxide nanoparticles [22, 23].

Marine macroalgae, particularly brown seaweeds, are recognized as reservoirs of diverse phytochemicals such as polyphenols, sulfated polysaccharides, terpenoids, and flavonoids [24-27]. These bioactives not only facilitate nanoparticle formation but also impart added therapeutic benefits, including anticancer, antimicrobial, and anti-inflammatory activities [28, 29]. *Turbinaria ornata*, a brown seaweed native to tropical marine habitats such as the Indian coastline, is one such promising source [30, 31]. Rich in phenolic compounds, alginates, and fucoidans, *T. ornata* offers a biocompatible and bioactive matrix for nanoparticle synthesis, further contributing to the functional efficacy of the resulting nanomaterials [32, 33].

In this study, we present the green synthesis of CuO NPs using aqueous extract of *T. ornata* and their subsequent integration into an electrospun composite nanoscaffold composed of starch and polyvinyl alcohol (PVA). The rationale for choosing starch and PVA as the scaffold matrix lies in their excellent biodegradability, biocompatibility, film-forming capability, and electrospinnability. While PVA contributes to mechanical strength and fiber formation, starch enhances porosity and provides additional biocompatible characteristics. The incorporation of CuO NPs synthesized from *T. ornata* adds an anticancer dimension to the scaffold, creating a multifunctional composite with potential applications in localized cancer therapy. The process of electrospinning was employed to fabricate nanofibrous scaffolds under optimized conditions, producing continuous and uniform nanofibers. Electrospinning not only enables the encapsulation of nanoparticles but also provides the flexibility to control fiber diameter, scaffold morphology, and surface characteristics. These parameters are critical for biomedical applications where cell adhesion, proliferation, and drug release kinetics are influenced by scaffold architecture. To validate the successful synthesis and incorporation of CuO NPs, a suite of physicochemical characterization techniques was utilized. UV-Vis spectroscopy confirmed the optical properties and surface plasmon resonance (SPR) of the synthesized nanoparticles. Fourier Transform Infrared Spectroscopy (FTIR) identified the functional groups involved in the reduction and stabilization processes. X-ray Diffraction (XRD) provided insights into the crystalline structure and phase purity of the nanoparticles. The morphological features and dispersion of CuO NPs within the nanofibers were evaluated using Scanning Electron Microscopy (SEM). Thermogravimetric Analysis (TGA) assessed the thermal stability of the composite scaffolds, while Dynamic Light Scattering (DLS) and zeta potential measurements determined particle size distribution and colloidal stability, respectively.

Beyond structural characterization, the biological efficacy of the fabricated scaffolds was explored through *in vitro* anticancer assays against two human cancer cell lines—HT-29 (colon adenocarcinoma) and MCF-7 (breast adenocarcinoma). The cytotoxic potential of the seaweed extract, CuO NPs, and composite nanoscaffolds was assessed using the MTT assay, a colorimetric technique widely employed for cell viability studies. The results are expected to reveal a dose-dependent anticancer effect, emphasizing the role of green-synthesized CuO NPs and their synergistic action when incorporated into biopolymer-based scaffolds. The novelty of this work lies in its holistic and green approach—from nanoparticle synthesis using marine macroalgae to the fabrication of electrospun nanoscaffolds with integrated anticancer potential. By leveraging naturally derived materials and eco-friendly processes, this study contributes to the growing field of sustainable nanomedicine. Furthermore, the dual functionality of the composite scaffolds—structural support with intrinsic bioactivity—positions them as attractive candidates for future translational research in localized cancer treatment, implantable drug delivery systems, or post-surgical therapeutic patches. Therefore, this study aims to bridge the domains of marine biotechnology, nanoscience, and biomedical engineering through the development of a starch/PVA/CuO-NP nanoscaffold synthesized via green chemistry. By combining the therapeutic properties of *T. ornata*-derived compounds with the structural advantages of electrospun nanofibers, the resultant composite offers a promising avenue for developing biocompatible, multifunctional materials tailored for advanced anticancer therapies.

2. MATERIALS AND METHODS

2.1. Chemicals and reagents

For the green synthesis of CuO NPs, *T. ornata* seaweed was collected from the coastal region of Rameswaram, Tamil Nadu, India. Copper (II) sulfate pentahydrate ($CuSO_4 \cdot 5H_2O$) from Sigma-Aldrich served as the copper precursor. PVA, with an estimated molecular weight of 115,000, functioned as the main polymer matrix in electrospinning. Starch sourced from a local vendor was incorporated to improve scaffold architecture. Analytical-grade solvents and chemicals, such as Milli-Q water and ethanol, were obtained from Merck and Sigma-Aldrich. The electrospinning process utilized a HOLMARC HO-NFES-040 unit with a precision-controlled syringe pump. Characterization tools included a VIS SPEC V-730 UV-Visible spectrophotometer, a PerkinElmer Spectrum Two FTIR spectrometer, a Bruker D8 Advance XRD unit, JEOL JSM-IT800 NANO SEM, a Malvern Zetasizer Ultra for DLS and zeta potential, and a PerkinElmer TGA 8000 for thermal assessment. HT-29 and MCF-7 cell lines

were obtained from the National Centre for Cell Science (NCCS), Pune, India, which provided authenticated and contamination-free cell stocks for biological investigations focused on anticancer activity.

2.2. Collection and processing of marine algae

T. ornata specimens were manually gathered from the nearshore waters of Rameswaram. The collected *T. Ornata* was taxonomically identified and authenticated by Dr V. Veeragurunathan, CSIR-CSMCRI-Marine Algal Research Station, Mandapam Camp 623519, Tamil Nadu, India. A voucher specimen was prepared and deposited at the Herbarium of the CSIR-CSMCRI-Marine Algal Research Station, under the accession number: SI–2025–RMM–022. This authentication ensures botanical accuracy and standardization of the study material. The seaweed was rinsed thoroughly with tap water to dislodge surface debris and subsequently washed several times using distilled water to eliminate salts and microcontaminants. Around 100 grams of the cleaned algae were finely chopped and subjected to air drying at ambient temperature for approximately 14 days. After complete dehydration, the material was ground into fine powder using a mechanical grinder and preserved in airtight containers for downstream extraction.

2.3. Extraction via ultrasonic treatment

To extract bioactive constituents, 2 grams of *T. ornata* powder were mixed with 50 mL of Milli-Q water in a sterile 100 mL beaker. This suspension underwent ultrasonic-assisted extraction at 60°C for 45 minutes using a LABQUEST ultrasonic cleaner (Borosil; Serial No. 941032329018). Following sonication, the extract was filtered under aseptic conditions using Whatman No. 1 filter paper. The clarified filtrate was stored at 10°C. For future applications, the extract was lyophilized to obtain a stable powdered form [34, 35].

2.4. Green synthesis of CuO NPs

Eco-conscious synthesis of CuO NPs involved combining 50 mL of 0.1 M $CuSO_4 \cdot 5H_2O$ with 10 mL of the seaweed extract (10 mg in 10 mL Milli-Q water) in a 5:1 volume ratio. The mixture was stirred at 650 rpm and kept at 60°C for two hours. A change in color from blue to bluish-green indicated nanoparticle formation. The product was centrifuged, rinsed thrice with double-distilled water, and subsequently freeze-dried over 48 hours to obtain nanopowder for further analysis [36].

2.5. Electrospinning of starch/PVA scaffolds loaded with CuO NPs

A 15% (w/w) aqueous solution of fully hydrolyzed PVA was prepared with continuous heating and stirring. Starch and synthesized CuO NPs (100 mg each) were added to the PVA solution and stirred at 50°C for 2.5 hours to ensure homogeneity. The mixture was loaded into a syringe with a 0.84 mm diameter needle and subjected to electrospinning using the HOLMARC HO-NFES-040 setup, powered by a HMPSKV30 power unit (0–30 kV, 0.5 mA). Optimal electrospinning conditions were: voltage 11.5 kV, needle-to-collector distance 12.3 cm, and feed rate 0.4 mL/h. Nanofiber mats were produced over 6–8 hours at room temperature [37-39].

2.6. Physicochemical characterization

2.6.1. UV–visible spectroscopy

Nanoparticle synthesis and optical characteristics were confirmed using a VIS SPEC V-730 spectrophotometer. Spectra for the seaweed extract, CuO NPs, and composite scaffolds were collected across 200–800 nm, with deionized water as reference. SPR peaks were indicative of successful nanoparticle formation [40].

2.6.2. FTIR spectroscopy analysis

FTIR spectra were acquired via a PerkinElmer Spectrum Two instrument in ATR mode over 4000–400 cm^{-1}, using 64 scans at a resolution of 4 cm^{-1}. Functional groups and molecular bonds in the extract, CuO NPs, and composite fibers were identified. Specific absorption bands for –OH, C=O, amide, and Cu–O vibrations confirmed material integration [41].

2.6.3. XRD analysis

Crystallinity of CuO NPs and composites was evaluated using a Bruker D8 Advance diffractometer employing CuKα radiation ($\lambda = 1.5406$ Å) at 40 kV and 40 mA. Scans from 5° to 90° (2θ) at 0.029649° intervals confirmed the monoclinic structure of CuO and its successful incorporation [42].

2.6.4. SEM analysis

Surface topography and distribution of nanoparticles were visualized using a JEOL JSM-IT800 NANO SEM. Samples were gold-coated to ensure conductivity. SEM images displayed fiber uniformity and effective dispersion of CuO NPs within the scaffold matrix [43].

2.6.5. TGA

Thermal characteristics of the composite mats were studied using a PerkinElmer TGA 8000 instrument. Approximately 5 mg of each sample was heated from ambient temperature to 550°C at 15°C/min in a nitrogen atmosphere. Thermograms revealed moisture loss, degradation phases, and overall thermal resilience [44].

2.6.6. Particle size and zeta potential

Particle size distribution and zeta potential were measured via Malvern Zetasizer Ultra. DLS quantified nanoparticle dimensions, while zeta potential values assessed colloidal stability. High absolute zeta potential values indicated good dispersion, crucial for biomedical applicability [45]. All data are publicly available in the Mendeley Data repository (DOI: 10.17632/tgxw2g4stx.1).

2.7. *In vitro* anticancer activity

2.7.1. Cell culture of HT-29 and MCF-7

HT-29 (human colon adenocarcinoma) and MCF-7 (breast cancer) cell lines were obtained from the National Center for Cell Science (NCCS), Pune. Cells were cultured according to NCCS guidelines using Minimum Essential Medium (MEM) supplemented with 10% fetal bovine serum (FBS) at 37°C in a 5% CO_2 incubator [28].

2.7.2. MTT assay for cell viability

Cells were seeded at 5×10^5 cells/well in 96-well plates and incubated overnight. Treatments included varying concentrations (6.25, 12.5, 25, 50, 100 µg/mL) of algal extract, CuO NPs, and starch/PVA/CuO nanoscaffolds in triplicates, followed by 24-hour incubation at 37°C with 5% CO_2. Post-incubation, MTT solution was added, and cells were incubated for an additional 4 hours. Formazan crystals were solubilized using 200 µL DMSO, and absorbance was read at 570 nm. The assay was repeated three times independently for accuracy. Results were reported as mean OD with standard deviations [46].

2.8. Statistical analysis

Data from triplicate experiments were analyzed using SPSS 25.0 and GraphPad Prism 9.0. Results were expressed as mean ± standard deviation. One-way ANOVA followed by appropriate post-hoc tests (Tukey's or Dunnett's) was used to evaluate group differences. A p-value < 0.05 was deemed significant. Pearson correlation assessed variable relationships, and the Shapiro-Wilk test evaluated normality. Logarithmic transformation was applied where normality assumptions failed. Analyses maintained a 95% confidence interval for data reliability [47].

3. RESULTS

3.1 UV–visible spectroscopy

The UV–Vis spectroscopic analysis (Fig. 1) revealed distinct optical properties for both *T. ornata* extract and the biosynthesized CuO NPs. The algal extract displayed a broad absorbance within the 200–400 nm wavelength range, with a prominent peak centered at approximately 346 nm and an absorbance intensity of 1.943. This absorption pattern suggests the presence of bioactive compounds such as chlorophyll derivatives, flavonoids, and phenolic substances. Conversely, the synthesized CuO NPs showed a narrow, intense absorption band near 200 nm, indicative of SPR associated with nanostructures. The spectral variation between the crude extract and the synthesized nanoparticles highlights successful nanoparticle formation and confirms the role of phytochemicals in nanoparticle stabilization and reduction. The incorporation of these nanostructures into nanofibrous scaffolds indicates potential for applications in ultraviolet filtration and photocatalysis.

3.2 FTIR spectroscopy analysis

FTIR spectroscopy (Fig. 2) verified the functional groups associated with both CuO NPs and the fabricated nanofibrous scaffolds. The CuO NPs showed distinct absorption peaks at 601 cm^{-1} (indicative of Cu–O bond stretching), 863 cm^{-1} (associated with metal–oxygen interactions), and 1061 cm^{-1} (C–O stretching vibrations). A broad absorption band around 3122 cm^{-1} was also observed, attributed to hydroxyl groups from adsorbed water or bioorganic capping agents. In the nanofiber spectrum, strong peaks appeared at 3284 cm^{-1} (O–H/N–H stretching), 2921 cm^{-1} (C–H bonds), and 1710 cm^{-1} (carbonyl group), confirming the presence of starch and PVA. Additional vibrations at 1328 cm^{-1} and 1087 cm^{-1} pointed to amine and glycosidic linkages. The coexistence of Cu–O signals with polymeric bands affirmed successful nanoparticle embedding without substantial chemical interaction between the components.

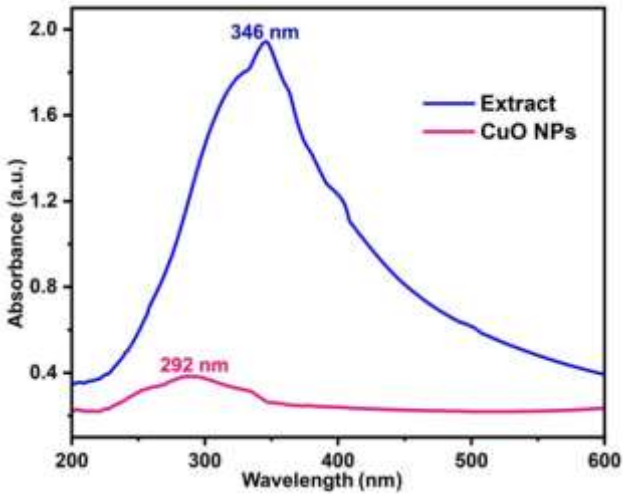

Fig. 1. UV–Visible spectral profiles of algal extract and CuO NPs.

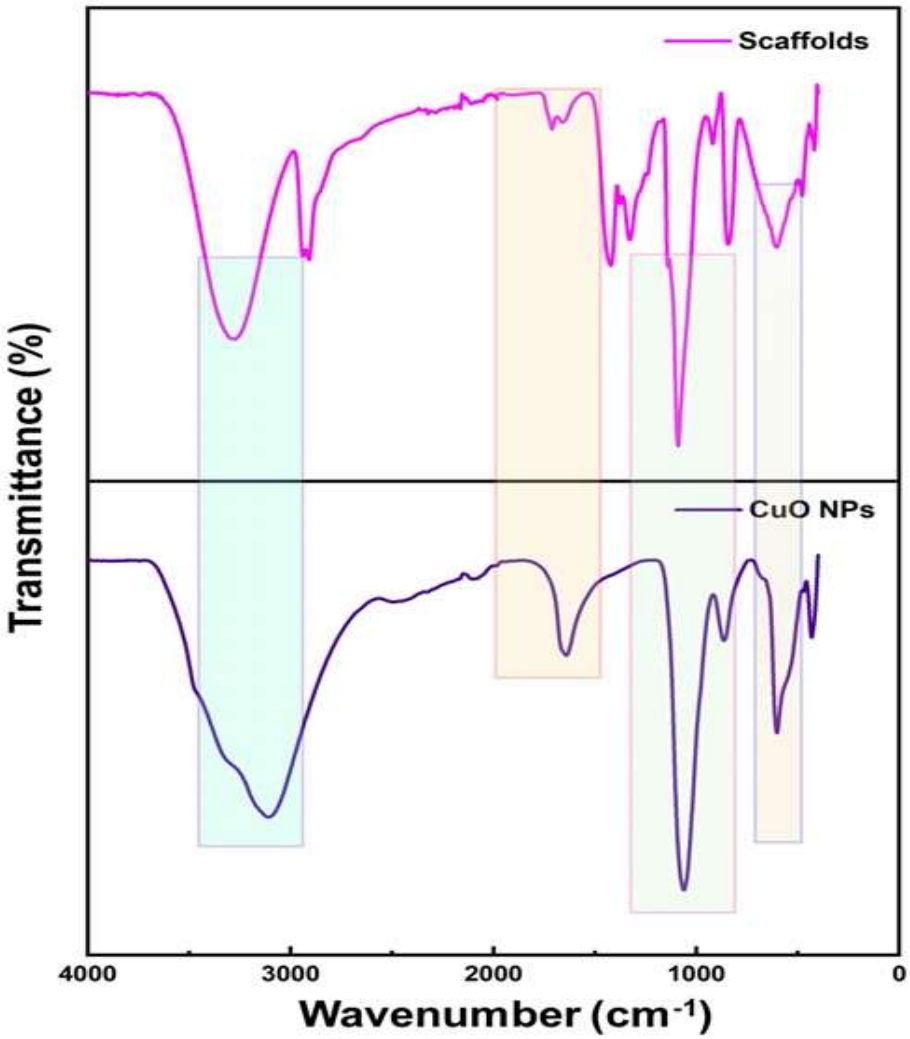

Fig. 2. FTIR spectra of CuO NPs and their incorporation into nanoscaffolds.

3.3 XRD analysis

XRD analysis (Fig. 3) established the crystallographic features of CuO NPs and their distribution in the nanofibrous structure. The diffraction profile of CuO NPs revealed 28 well-defined peaks in the 2θ range from 5° to 90°, with intense reflections at 24.435°, 32.876°, and 38.504°, corresponding to monoclinic CuO, matching the JCPDS card No. 48-1548. In contrast, the nanofibrous scaffolds exhibited broader and less sharp peaks, with major reflections at 21.420°, 29.372°, and 57.572°, indicating reduced crystallinity due to polymer matrix interference. The overall crystallinity index of the scaffold was calculated to be 17.4%. The broader peaks and minor angular

shifts suggest polymer-induced amorphization and confirm the effective dispersion of nanoparticles within the nanoscaffold network.

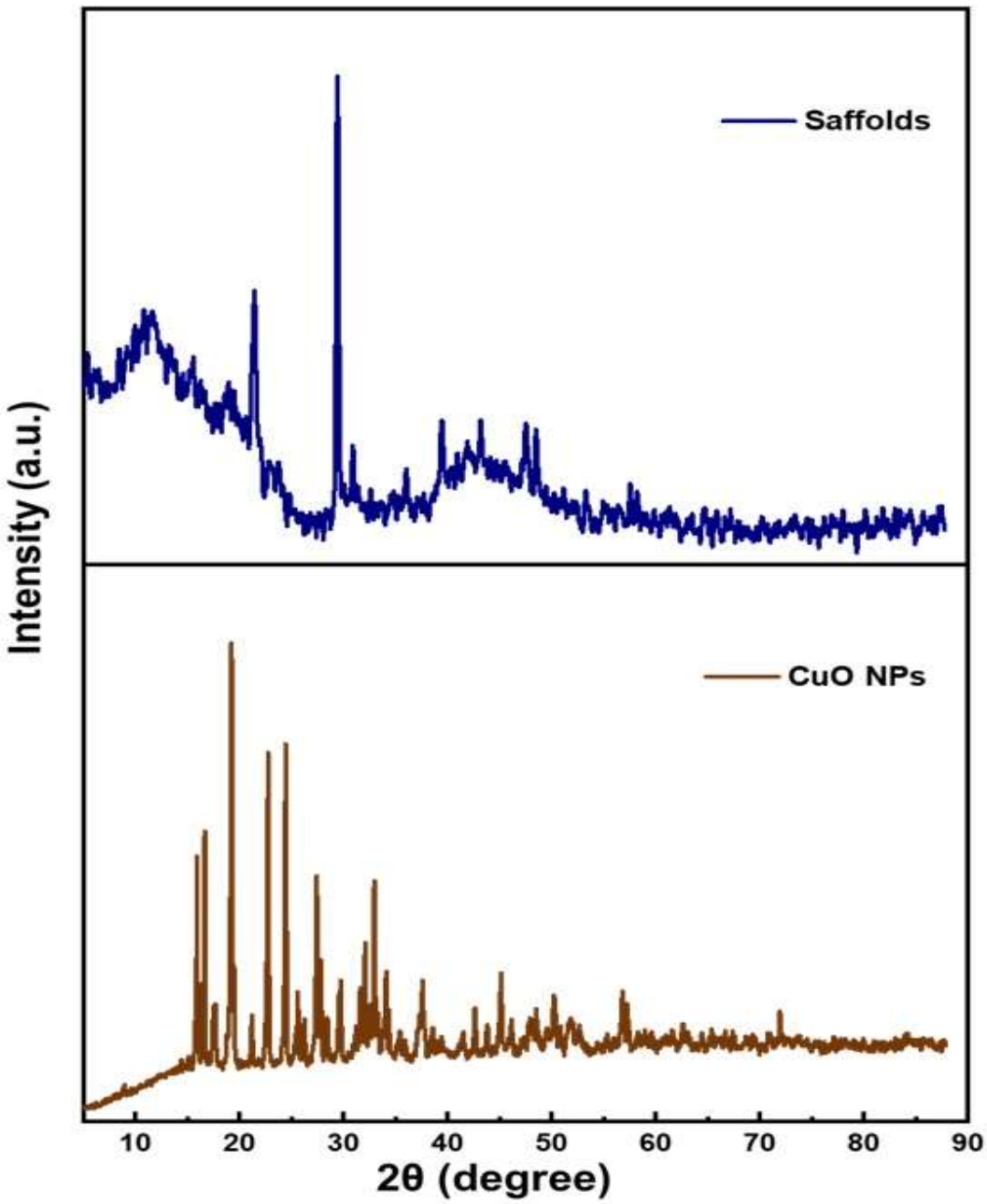

Fig. 3. XRD patterns of synthesized CuO NPs and CuO-loaded scaffolds.

3.4 SEM analysis

SEM (Fig. 4) provided insights into the morphology of both CuO NPs and the electrospun nanofibrous mats. The nanoparticles were predominantly spherical to irregular, measuring between 90–100 nm, with slight aggregation attributed to high surface energy. The starch/PVA nanofibers exhibited smooth, bead-free surfaces with diameters ranging from 150–300 nm. Embedded nanoparticles were uniformly distributed along the fiber surfaces, with minimal clumping. Some larger clusters were occasionally visible, likely due to interfacial forces between particles and the polymer. The nanofibers formed a porous, interconnected network ideal for biomedical applications. These micrographs confirm that the nanoparticles were successfully synthesized and effectively integrated into the fibrous structure, though dispersion uniformity could still be improved.

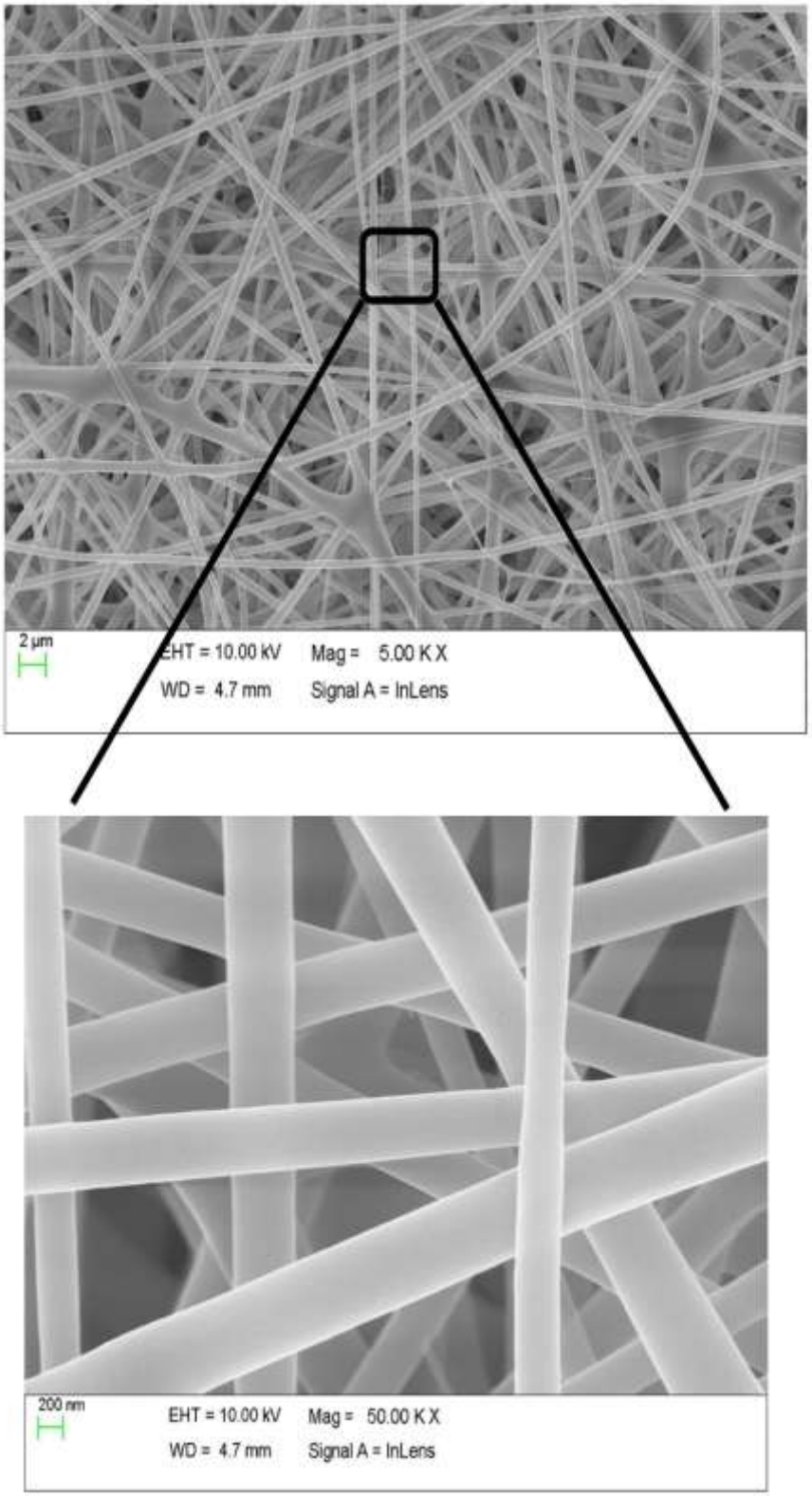

Fig.4. SEM analysis of starch/PVA/CuO-NPs nanoscaffolds

3.5 TGA

Thermal stability of the nanofibrous scaffold incorporating CuO NPs was evaluated through TGA (Fig. 5). A 2.315 mg sample was subjected to heating from 30°C to 550°C at a 15°C/min ramp under a nitrogen environment. The first weight loss phase (9.509%) was noted due to moisture and volatile substance evaporation. Decomposition of the polymer matrix began around 244.81°C, peaked at 332.83°C, and ended by 378.85°C. The total mass loss at 550°C was recorded at 41.696%. Compared to the pristine polymer, the presence of CuO NPs delayed the thermal degradation onset and improved thermal resistance. This enhancement indicates the nanoparticles' role in reinforcing the polymer matrix and improving heat endurance.

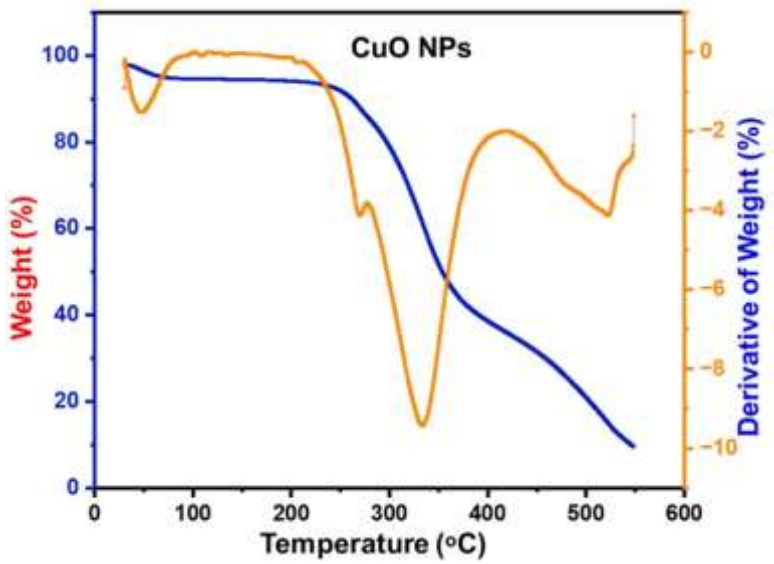

Fig. 5. Thermal degradation behavior of CuO-incorporated nanoscaffolds.

3.6 Zeta potential and particle size distribution

DLS analysis determined the particle size and colloidal stability of CuO NPs. The particles displayed a bimodal size distribution, with a mean hydrodynamic diameter of 92.8 nm and a polydispersity index (PDI) of 0.5592, indicating moderate size dispersion (Fig. 6). The count rate observed was 3465 kcps, suggesting a reasonably stable suspension during measurement. Zeta potential was recorded at –5.29 mV (Fig. 7), reflecting low electrostatic repulsion and suggesting limited colloidal stability. This low surface charge corresponds with aggregation tendencies observed under SEM. To improve long-term dispersion, surface functionalization techniques may be necessary to prevent nanoparticle clustering in biological or environmental settings.

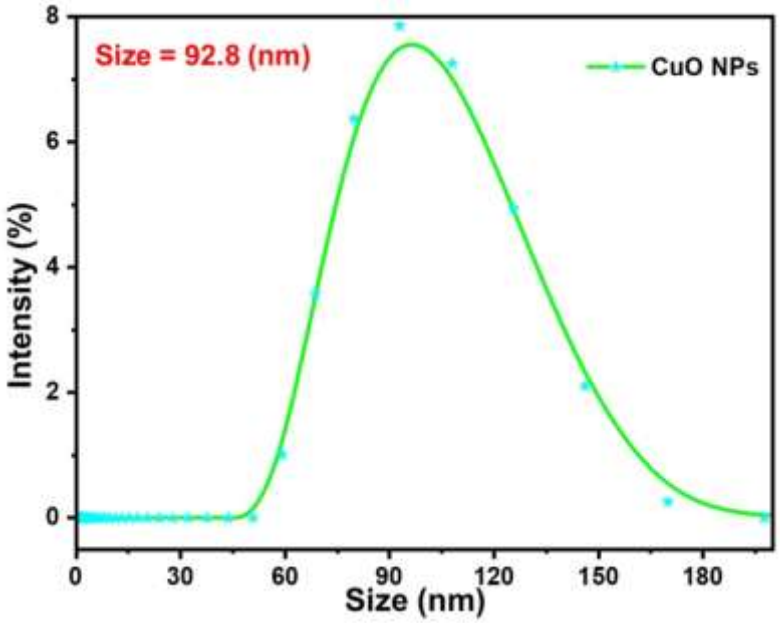

Fig.6. DLS particles size analysis of CuO NPs

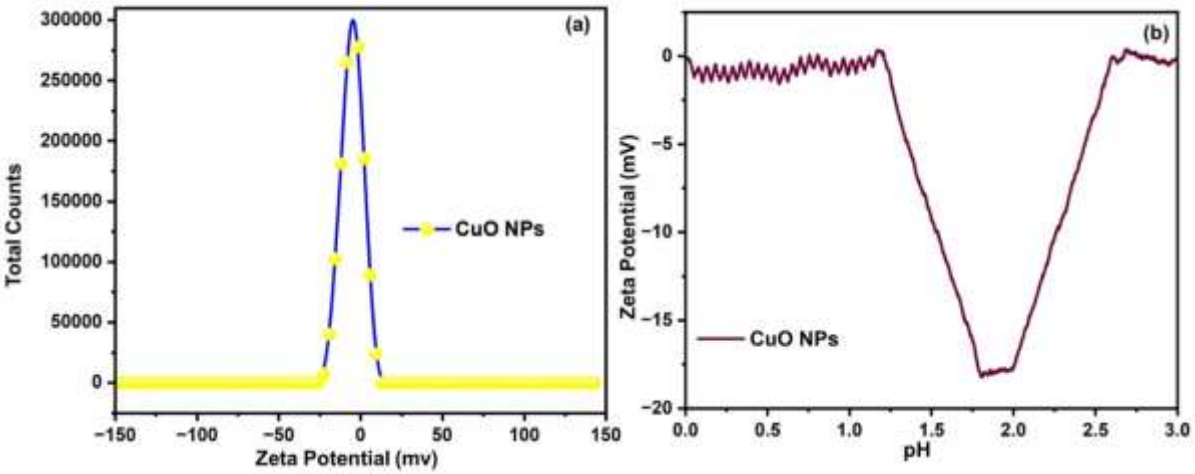

Fig.7. Zeta-potential analysis of CuO NPs

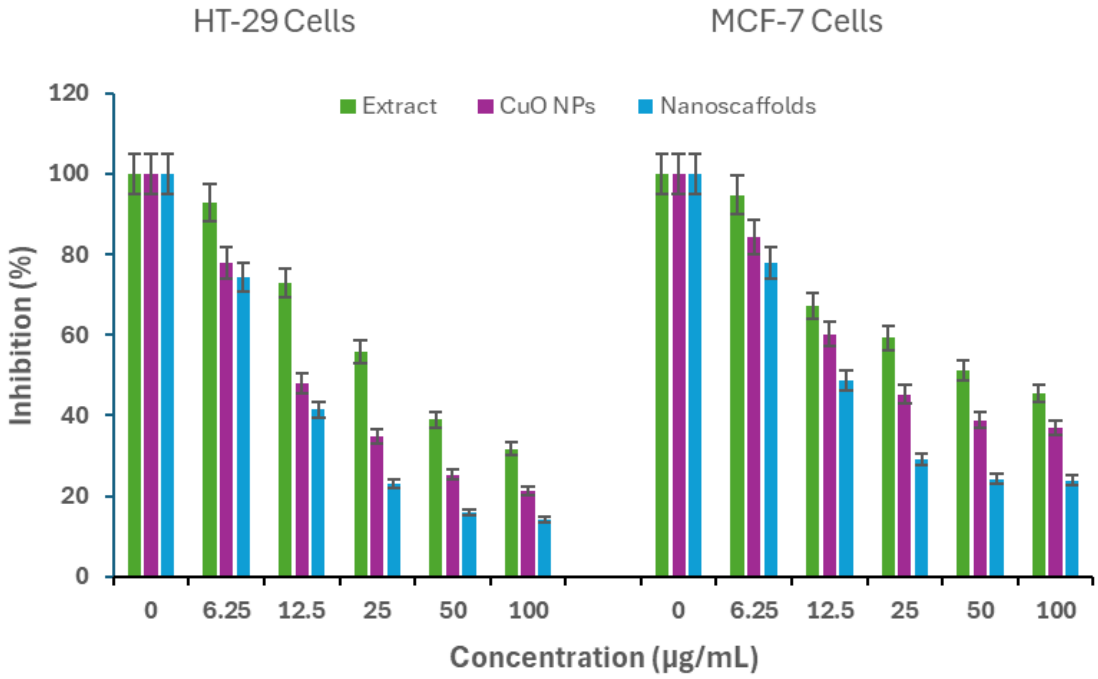

Fig.8. Anticancer activity analysis of algal extract, CuNPs and starch/PVA/CuONPs nanoscaffolds.

3.7. Evaluation of anticancer activity

The results demonstrated a dose-dependent reduction in cell viability for all tested compounds—algal extract, CuO NPs, and starch/PVA/CuO-NPs nanoscaffolds—against both HT-29 (colon cancer) and MCF-7 (breast cancer) cell lines. In HT-29 cells, the algal extract exhibited moderate cytotoxicity, reducing cell viability to 31.65% at the highest concentration (100 µg/mL). The inhibitory effect was concentration-dependent, with viability decreasing to 38.9% (50 µg/mL), 55.9% (25 µg/mL), and 72.9% (12.5 µg/mL). The IC_{50} (half-maximal inhibitory concentration) was estimated at ~45 µg/mL, indicating moderate anticancer activity. In contrast, CuO NPs demonstrated stronger cytotoxicity, lowering viability to 21.23% at 100 µg/mL, with an IC_{50} of ~30 µg/mL, suggesting enhanced potency compared to the algal extract. The most effective treatment was the starch/PVA/CuO-NPs nanoscaffolds, which reduced cell viability to 14.28% at 100 µg/mL and exhibited the lowest IC_{50} (~20 µg/mL), highlighting their superior anticancer potential. A similar trend was observed in MCF-7 cells, where the algal extract reduced viability to 45.45% at 100 µg/mL, with an IC_{50} of ~55 µg/mL, indicating weaker activity compared to its effects on HT-29 cells. CuO NPs showed improved efficacy, decreasing viability to 36.87% at the highest concentration and an IC_{50} of ~40 µg/mL. Once again, the starch/PVA/CuO-NPs nanoscaffolds outperformed the other treatments, achieving 23.82% viability at 100 µg/mL and an IC_{50} of ~25 µg/mL, reinforcing their enhanced cytotoxic effect. The starch/PVA/CuO-NPs nanoscaffolds exhibited the strongest anticancer activity against both HT-29 and MCF-7 cell lines, as evidenced by their significantly lower

IC_{50} values compared to CuO NPs and algal extract alone. This enhanced efficacy may be attributed to the synergistic effects of the nanocomposite structure, which improves drug delivery and cellular uptake. The findings suggest that these nanoscaffolds hold promise as a potential therapeutic agent for colon and breast cancer treatment. However, further research is necessary to elucidate their precise mechanisms of action and evaluate their safety and efficacy in *in vivo* models.

4. DISCUSSION

The characterization and biological evaluation of CuO NPs synthesized using *T. ornata* extract and their incorporation into starch/PVA nanofibrous scaffolds revealed promising physicochemical and anticancer properties. The study's findings validate the potential of green-synthesized nanomaterials for biomedical applications, particularly in cancer therapy, through the use of environmentally benign methods and biodegradable polymers.

UV–Visible spectroscopy provided the first evidence of successful nanoparticle synthesis. The algal extract displayed a broad absorbance spectrum, with a significant peak at 346 nm, which may be attributed to naturally occurring phytochemicals like flavonoids, chlorophyll derivatives, and phenolic compounds. These biomolecules likely functioned as reducing and capping agents during the biosynthesis of CuO NPs. The strong absorbance peak near 200 nm in the CuO NPs confirmed their formation and the presence of SPR, a signature phenomenon of metal oxide nanostructures. The spectral distinction between the extract and the nanoparticles further underscores the transformation mediated by phytoconstituents, suggesting their integral role in nanoparticle nucleation and stabilization [48-52].

FTIR spectroscopy further confirmed the involvement of functional groups from the *T. ornata* extract in nanoparticle synthesis and stabilization. The characteristic bands at 601 cm^{-1} and 863 cm^{-1} in CuO NPs indicated Cu–O bond vibrations, while broader absorption around 3122 cm^{-1} suggested hydroxyl groups possibly derived from bio-organic compounds on the nanoparticle surface. In the composite nanofibers, additional peaks corresponding to O–H/N–H, C–H, and carbonyl groups validated the presence of starch and PVA. The combination of Cu–O peaks with polymer-associated bands confirmed successful nanoparticle incorporation without major chemical interaction, indicating that the nanoparticles were physically embedded and retained their identity within the polymer matrix [53, 54].

XRD analysis corroborated the crystalline nature of the synthesized CuO NPs. Peaks matching monoclinic CuO confirmed phase purity and crystallinity. The reduction in crystallinity observed in nanofiber scaffolds, with broader peaks and decreased intensity, is attributed to the amorphous nature of the polymeric blend and uniform nanoparticle dispersion. The calculated crystallinity index of 17.4% implies that while the nanoparticles retained their structure, the polymer matrix interfered with long-range ordering, thereby promoting amorphization. Such partial amorphization can be beneficial for biomedical applications, as it often enhances drug release and cellular interactions [55-58].

SEM revealed the morphological features of both CuO NPs and nanofibers. The nanoparticles, ranging from 90–100 nm, appeared spherical with minor aggregation, potentially due to van der Waals interactions. The starch/PVA nanofibers had smooth, continuous surfaces with an average diameter of 150–300 nm and exhibited uniform nanoparticle distribution. Occasional nanoparticle clustering was visible but did not disrupt the fibrous network. The formation of a porous and interconnected matrix is advantageous for applications like drug delivery and tissue engineering, where diffusion and cell infiltration are critical [59-62].

TGA demonstrated the thermal enhancement conferred by CuO NP incorporation. The scaffold showed three distinct weight-loss stages, with the most significant polymer degradation occurring between 244°C and 378°C. The delayed onset of decomposition, as compared to native polymeric blends, highlights the stabilizing role of CuO NPs within the scaffold. This enhanced thermal resistance can be attributed to the strong interaction between the nanoparticles and the polymer chains, which likely restricts molecular motion and hinders thermal degradation [63, 64].

The zeta potential and DLS analyses offered insight into the colloidal stability and size distribution of CuO NPs. A bimodal size distribution centered around 92.8 nm and a moderate polydispersity index indicated reasonably uniform particles. However, the zeta potential of –5.29 mV suggested low electrostatic repulsion, predisposing the particles to mild aggregation—a finding corroborated by SEM. For future applications, improving colloidal stability through surface modification or functionalization could significantly enhance dispersion in biological systems, potentially improving therapeutic efficacy [65-69].

Crucially, the *in vitro* cytotoxicity assays against HT-29 (colon cancer) and MCF-7 (breast cancer) cell lines highlighted the anticancer potential of the nanoscaffolds. The algal extract exhibited moderate cytotoxicity, with IC_{50} values of ~45 µg/mL for HT-29 and ~55 µg/mL for MCF-7, likely due to the presence of bioactive metabolites. CuO NPs demonstrated improved cytotoxicity, indicating their intrinsic pro-oxidative and apoptotic-inducing

properties. The starch/PVA/CuO-NPs nanoscaffolds showed the most potent anticancer effects, with IC_{50} values of ~20 µg/mL and ~25 µg/mL for HT-29 and MCF-7, respectively. This enhanced efficacy is likely due to the synergistic action between the nanocarrier and the nanoparticles, which facilitates better cellular uptake and sustained release of cytotoxic agents. The superior performance of the nanoscaffolds also points to the scaffold's potential role in overcoming multidrug resistance by improving drug delivery efficiency [70, 71].

The biosynthesized CuO NPs and their incorporation into starch/PVA nanofibrous scaffolds present a promising platform for cancer therapy. The green synthesis approach, combined with the enhanced physicochemical and biological properties of the nanocomposite, offers a sustainable and effective strategy for anticancer applications. However, to advance toward clinical translation, further investigations involving mechanistic cellular studies, biodistribution profiling, and *in vivo* efficacy assessments are essential.

5. CONCLUSION

The present study successfully demonstrated the eco-friendly synthesis of CuO NPs using *T. ornata* extract and their effective incorporation into starch/PVA-based nanofibrous scaffolds. Comprehensive characterization confirmed the structural, morphological, and thermal integrity of the nanocomposite system. UV–Vis and FTIR analyses validated nanoparticle formation and phytochemical capping, while XRD and SEM analyses revealed uniform dispersion of CuO within the nanofibrous matrix. Thermal analysis indicated improved heat resistance due to nanoparticle reinforcement. Moreover, DLS and zeta potential assessments provided insights into the colloidal behavior of the synthesized nanoparticles. Importantly, the anticancer evaluation revealed a significant, dose-dependent cytotoxic effect, with the starch/PVA/CuO nanoscaffolds exhibiting superior activity against HT-29 and MCF-7 cell lines compared to CuO NPs and algal extract alone. These findings underscore the potential of this nanofibrous system as a promising candidate for targeted cancer therapy. Further *in vivo* studies are warranted to validate its therapeutic efficacy and biocompatibility.

Data Availability Statement: The full dataset of physiochemical characterization associated with this work is published in Mendeley Data [Dataset] Eco-friendly nanocomposite scaffolds: physicochemical analysis of starch matrices integrated with *Turbinaria ornata*-mediated CuO nanoparticles (DOI: 10.17632/tgxw2g4stx.1). **Disclosure:** The material characterization data and figures (e.g., UV, SEM, FTIR, XRD, TGA, Zeta Potential and particle sizer) presented here were generated from a common dataset and are being reused across multiple related studies on nanomaterials. All biological analyses and conclusions are original to each manuscript.

Conflicts of Interest: The authors declare no conflicts of interest.

REFERENCES

[1] Guan T, Gong J, Lin J, Palanisamy CP, Jinjin Pei J, El-Aty AMA. Machine learning-driven multimodal optimization of selenium biotransformation and flavor profiling in fermented apple–Yacon functional beverages. Innovative Food Science & Emerging Technologies. 2025; 105: 104198.

[2] Natarajan SR, Krishnamoorthy R, Alshuniaber MA, Alsulami TS, Gatasheh MK, Rajagopal P, Palanisamy CP, Govindan R, Veeraraghavan VP, Jayaraman S. ABCE1 facilitates tumour progression via aerobic glycolysis and inhibits cell death in human colorectal cancer cells through the p53 signalling pathway. Scientific Reports. 2025; 15: 24674.

[3] Huang Y, Guo H, Liu Y, Jin W, Palanisamy CP, Pei J, Oz F, El-Aty AMA. Effects of Natural Polysaccharides on the Gut Microbiota Related to Human Metabolic Health. Molecular Nutrition & Food Research. 2025; 69:e202400792.

[4] Poornima K, Meenakshi K.C, Manikandan V.R, Shankari G, Prabhu D, Rathi M.A, Palanisamy CP, Balaji R, Gopalakrishnan V.K. Exploring the anticancer potential of Jerantinine A from *Tabernaemontana coronaria* against prostate, breast, and ovarian cancers: A computational approach. *Journal of Complementary and Integrative Medicine*, 2025 22(2): 363–372.

[5] Palanisamy CP, Poompradub S, Sansanaphongpricha K, Jayaraman S, Subramani K. Faridah Sonsudin gGreen synthesis of Nigella sativa-mediated silver nanoparticles for enhanced antibacterial activity and wound healing: Mechanistic insights and biomedical applications. Environmental Nanotechnology, Monitoring & Management. 2025; 24: 101085.

[6] Surendran N, Raju MV, Chandrasekaran MK, Ahalliya RM, Palanisamy CP, Chandrasekaran G, Kanniappan GV. Physicochemical characterization of starch from Maranta arundinacea L.(arrowroot) rhizomes and its inhibition of COX-2: In vivo validation. Bioactive Carbohydrates and Dietary Fibre. 2025; 33: 100465.

[7] Kannappan P, Chandrasekaran MK, Raju MV, Gopalakrishnan S, Dhamodharan P, Ahalliya RM, Palanisamy CP, Raju B, Kanniappan GV. Exploring the anticancer potential of Jerantinine A from Tabernaemontana

coronaria against prostate, breast, and ovarian cancers: a computational approach. Journal of Complementary and Integrative Medicine. 2025; 22(02): 363-372.

[8] Pei J, Kumarasamy RV, Jayaraman S, Kanniappan GV, Long Q, Palanisamy CP. Quercetin-functionalized nanomaterials: Innovative therapeutic avenues for Alzheimer's disease management. Ageing Research Reviews. 2025; 104: 102665.

[9] Jayaraman S, Prasad M, Natarajan SR, Krishnamoorthy R, Alshuniaber MA, Gatasheh MK, Veeraraghavan VP, Rajagopal P, Palanisamy CP. Molecular mechanisms underlying the effects of beta-sitosterol on TGF-β1/Nrf2/SIRT1/p53-mediated signaling in the kidney of a high-fat diet and sucrose-induced type-2 diabetic rat. Chemico-Biological Interactions. 2025; 411: 111443.

[10] Huang Y, Guo H, Liu Y, Jin W, Palanisamy CP, Pei J, Oz F, El-Aty AMA. Effects of Natural Polysaccharides on the Gut Microbiota Related to Human Metabolic Health. Molecular Nutrition & Food Research. 2025; e202400792.

[11] Prabhakaran P, Palanisamy CP, Shanmugam A, Damodharan P, Swaminathan H, Devaraj D, Ahalliya RM, Kanniappan GV. Isolation, structural characterization, and molecular docking studies on the bioactive compound from n-Hexane extract of Emilia sonchifolia (L.) DC against the pancreatic cancer target Aurora 2 Kinase. Journal of Complementary and Integrative Medicine. 2024; 22(1): 0290.

[12] Jiang H, Kumarasamy RV, Pei J, Raju K, Kanniappan GV, Palanisamy CP. Integrating engineered nanomaterials with extracellular vesicles: Advancing targeted drug delivery and biomedical applications. Frontiers in Nanotechnology. 2024; 6: 1513683.

[13] Guo H, Liu Y, Wan T, Song D, Palanisamy CP, Geng J, Pei J, Özmen S, El-Aty AMA. Toward personalized cancer management: Role of precision nutrition–diet interventions. Journal of Functional Foods. 2024; 123: 106584.

[14] Natarajan SR, Krishnamoorthy R, Alshuniaber MA, Al-Anazi KM, Farah MA, Rajagopal P, Palanisamy CP, Veeraraghavan VP, Jayaraman S. Identification of FOXM1 as a novel protein biomarker and therapeutic target for colorectal cancer progression: Evidence from immune infiltration and bioinformatic analyses. International Journal of Biological Macromolecules. 282 (Part 4): 137201.

[15] Rajendran MS, Jayaraman S, Khan JM, Jasmine S, Prabhakaran RK, Raju MV, Chandrasekaran MK, Ahalliya RM, Kannappan P, Palanisamy CP, Kanniappan GV. Investigating the colon toxicity and carcinogenic role of monosodium glutamate compared with Dimethylhydrazine in male Wistar rats: Exploring the link to childhood colon cancer risk. Journal of King Saud University - Science. 2024; 36(11): 103507.

[16] Kumarasamy RV, Natarajan P, Umapathy VR, Roy JR, Rab SO, Saeed M, Panagal M, Mironescu M, Srinivasan GP, Palanisamy CP. Clinical Applications and Therapeutic Potentials of Advanced Nanoparticles: A Comprehensive Review on Completed Human Clinical Trials. Frontiers in Nanotechnology. 2024; 6:1479993.

[17] Jin W, Pei JJ, Roy JR, Jayaraman S, Ahalliya RM, Kanniappan GV, Mironescu M, Palanisamy CP. Comprehensive review on single-cell RNA sequencing: A new frontier in Alzheimer's disease research. Ageing Research Reviews. 2024; 274: 102454.

[18] Pei J, Palanisamy CP, Jayaraman S, Natarajan PM, Umapathy VR, Roy JR, Panagal M, Jayaraman S. Curcumin-loaded polymeric nanomaterials as a novel therapeutic strategy for Alzheimer's disease: A comprehensive review. Ageing Research Reviews. 2024; 99: 102393.

[19] Pei J, Palanisamy CP, Jayaraman S, Natarajan PM, Umapathy VR, Roy JR, Thalamati D, Ahalliya RM, Kanniappan GV, Mironescu M. A comprehensive review on starch-based Sustainable Edible Films Loaded with Bioactive Components for Food Packaging. International Journal of Biological macromolecules. 2024; 274 (Part-1): 133332.

[20] Umapathy V, Dhanavel A, Kesavan R, Natarajan PM, Bhuminathan S, Vijayalakshmi P. Anticancer Potential of the Principal Constituent of Piper nigrum, Piperine: A Comprehensive Review. Cureus. 2024; 16(2): e54425.

[21] Umapathy VR, Swamikannu B, Natarajan PM, Devi R, Nandini MS, Vimalarani, Vijayalakshmi P. In Silico Molecular Docking of Ocimum sanctum Phytochemicals: Targeting Key Biomarkers in Oral Cancer. Journal of Pharmacy and Bioallied Sciences. 2024; 16(5): S4792-S4799.

[22] Swamikannu B, Umapathy VR, Natarajan PM, Nandini MS, Stylin AGSQ, Vimalarani V, Rajinikanth S. Unlocking the Therapeutic Benefits of Artemisia Annua: A Comprehensive Overview of its Medicinal Properties. Journal of Pharmacy and Bioallied Sciences. 2024; 16(5): S4248-S4253.

[23] Yadalam PK, Arumuganainar D, Natarajan PM, Ardila CM. Artificial intelligence-powered prediction of AIM-2 inflammasome sequences using transformers and graph attention networks in periodontal inflammation. Scientific Reports. 2025; 15: 8733.
[24] Yadalam PK, Chatterjee S, Natarajan PM, Ardila CM. Comparison of light gradient boosting and logistic r egression for interactomic hub genes in Porphyromonas gingivalis and Fusobacterium nucleatum-induced periodontitis with Alzheimer's disease. Frontiers in Oral Health. 2025; 6:1463458.
[25] Yadalam PK, Natarajan PM, Ardila CM. Variational graph autoencoder for reconstructed transcriptomic data associated with NLRP3 mediated pyroptosis in periodontitis. Scientific Reports. 2025; 15: 1962.
[26] Daniel Raja FS, Abraham L, Rangasamy K, Saikia K, Rathankumar AK, Mironescu M, Mironescu I, Palanisamy CP, Kanniappan GV. Next-Generation Microbiome Therapeutics: Psychobiotics and Fecal Microbiota Transplants (FMT) for Mental Health Treatment. Frontiers in Cellular and Infection Microbiology. 2026; 16: 1719357.
[27] Dharmaprakash S, Gunasekaran VP, Sivaramakrishnan R, Kanniappan GV, Jayaraman S, Mironescu M, Rajabathar JR, Mironescu ID, Palanisamy CP. Marine macroalgae-mediated ultrasonic-assisted green synthesis of CuO nanoparticles embedded in starch/PVA electrospun nanoscaffolds for in vitro α-amylase and α-glucosidase inhibitory activity. Scientific Reports. 2026.
[28] Surendran N, Chandrasekaran G, Raju MV, Chandrasekaran MK, Ahalliya RM, Palanisamy CP, Kanniappan GV, Arcot R, Alharbi NS, Thiruvengadam M. Anti-inflammatory potential of ethanolic extract of Maranta arundinacea L.: Insights from COX-2 modulation and oxidative stress analysis. South African Journal of Botany. 2026; 195: 142-151.
[29] Pei J, Senthilkumar MV, Hessini K, Subramaniyam S, Sivaramakrishnan R, Kanniappan GV, Jayaraman S, Palanisamy CP. Green fabrication of starch/PVA/CuO nanoscaffolds using marine macroalgae extract for enhanced anti-inflammatory activity. Sustainable Chemistry and Pharmacy. 2026; 51: 102397.
[30] Balasubramanian V, Loganathan L, Muthuswamy K, Viswanathan TM, Raju MV, Chandrasekaran MK, Ahalliya RM, Poorasamy J, Palanisamy CP, Dominic S, Kanniappan GV. Anticancer therapeutic efficacy of PEGylated β-galactosidase from Aspergillus terreus in DMBA-induced breast cancer: Toxicological, molecular and histopathological evaluation in Wistar rats. International Journal of Biological Macromolecules. 2026; 360: 151856.
[31] Jayaraman S, Eswaran A, Rajagopal P, Palanisamy CP, Veerakumar P, Veeraraghavan VP, Sirasanagandla SR. Neuroendocrine-associated epigenetic factors in cellular senescence: mechanisms and therapeutic implications. Biogerontology. 2026; 27(2): 64.
[32] Ponnusamy B, Rajagopal P, Palanisamy CP, Veeraraghavan VP, Jayaraman S. Mechanistic Exploration of the anticancer activity of Justicia adhatoda Plant Leaf Ethanolic Extract against Colon Cancer Cells: An in silico and in vitro Approach. Asian Pacific Journal of Cancer Prevention. 2026; 27(3): 1069-1080.
[33] Pei J, Saran VS, Sivaramakrishnan R, Kanniappan GV, Pandurangan V, Jayaraman S, Dhayalan VK, Mironescu M, Mironescu ID, Palanisamy CP. Ultrasonic-assisted, Sargassum ilicifolium (brown marine macroalgae)-mediated biogenic synthesis of CuO nanoparticles incorporated in starch/PVA electrospun nanoscaffolds: In vitro safety and antioxidant efficacy assessment. Bioorganic Chemistry. 2026; 173: 109679.
[34] Raj MAPA, Subramaniyam S, Kanniappan GV, Jayaraman S, Palanisamy CP. Sustainable fabrication of starch/PVA/CuO electrospun nanoscaffolds from Turbinaria ornata (marine macroalgae) extract: Physicochemical characterization and antidiabetic evaluation. Kuwait Journal of Science. 2026; 53(2): 100545.
[35] Pei J, Ganesh NS, Subramaniyam S, Sivaramakrishnan R, Kanniappan GV, Jayaraman S, Palanisamy CP. Sustainable fabrication of starch/PVA/CuO electrospun nanoscaffolds from Padina tetrastromatica (Brown macroalgae) extract: Physicochemical characterization and antidiabetic assessment. Sustainable Chemistry One World. 2026; 9: 100195.
[36] Sakthiraj A, Sivaramakrishnan R, Subramaniyam S, Kanniappan GV, Pandurangan V, Jayaraman S, Dhayalan VK, Mironescu M, Mironescu ID, Palanisamy CP. Starch/PVA electrospun nanoscaffolds loaded with ultrasonic-assisted green-synthesis of CuO nanoparticles from marine macroalgae (Gracilaria corticata) extract: Cytotoxicity and antioxidant analysis. Chemical Physics Impact. 2026; 12: 101018.
[37] Raju M, Chandrasekaran MK, Loganathan L, Ahalliya RM, Mironescu M, Mironescu ID, Palanisamy CP, Kanniappan GV. Lipid remodeling and ferroptosis in phosphatidylcholine-mediated tumor–stroma crosstalk. Frontiers in Molecular Biosciences. 2026; 13: 1742305.
[38] Kunamalla R, Panagal M, Palanisamy CP. Biogenic synthesis and fabrication of starch/PVA/CuO electrospun nanoscaffolds from Sargassum ilicifolium (brown marine macroalgae) extract for anticancer activity on HT-29 and MCF-7 cancer cells. Biocatalysis and Agricultural Biotechnology. 2026; 72: 103923.

[39] Pei J, Govindaraj H, Sivaramakrishnan R, Kanniappan GV, Pandurangan V, Dhayalan VK, Mironescu M, Mironescu ID, Jayaraman S, Palanisamy PC. Sustainable fabrication of biopolymer-based (starch/PVA) nanoscaffolds loaded with green-synthesized CuO nanoparticles from Sargassum wightii (marine macroalgae): Cytocompatibility and antioxidant activity. Biomaterials Advances. 2026; 182: 214660.
[40] Pei J, Perumal NC, Meng P, Long Q, Palanisamy CP. Extracellular vesicle-based biosensors for Alzheimer's disease: A new frontier in precision diagnostics. Ageing Research Reviews. 2026; 113: 102904.
[41] Shree P, Sivaramakrishnan R, Kanniappan GV, Pandurangan V, Jayaraman S, Dhayalan VK, Mironescu M, Mironescu ID, Palanisamy CP. Antioxidant and biocompatible CuO-starch/PVA nanoscaffolds via ultrasonic green synthesis using Turbinaria conoides (brown marine macroalgae). Medicine in Drug Discovery. 2025; 28: 100238.
[42] Gong J, Lin J, Guan T, Pei J, Palanisamy CP, El-AtyFrom AMA. selenium tolerance to nanoplastic antagonism: Comprehensive characterization of L. casei SNUT1 and its extracellular vesicle–nanoselenium complex. Food Bioscience. 2025; 74: 107749.
[43] Poochi SP, Sundarraj R, Raju MV, Chandrasekaran MK, Ahalliya RM, Palanisamy CP, Kanniappan GV, Kondapavuluri BK, Thiruvengadam M. Harnessing Nature: Computational and Experimental Insights Into *Ipomoea obscura* Metabolites for Bladder Cancer Therapy. Chemistry and Biodiversity. 2025; 0: e00909.
[44] Dugganaboyana GK, Kannankumar MKG, Shivaramakrishna S, Raju MV, Chandrasekaran MK, Ahalliya RM, Panneerselvam N, Palanisamy CP, Kanniappan GV. Phytochemical insights, antioxidant activity and therapeutic potential of Cassia senna against prostate cancer in Wistar albino rats. Discover Applied Sciences. 2025; 7:1206.
[45] Natarajan SR, Krishnamoorthy R, Alshuniaber MA, Gatasheh MK, Rajagopal P, Veeraraghavan VP, Palanisamy CP, Jayaraman S. KDM1A Facilitates Oncogenic Potential in Colorectal Cancer Progression Through the Activation of AXIN/GSK3β/β-Catenin Signaling Pathways: Evidence From Integrated Transcriptomics and In Vitro Studies. The Journal of Gene Medicine. 2025; 27(11): e70053.
[46] Natarajan PM. Dental Bioinformnatics-Current Scope and Future perspectives. Research Journal of Pharmacy and Technology. 2022;15(5):2351-6.
[47] Natarajan PM, Umapathy VR, Murali A, Swamikannu B. (2022). Computational Simulations of Identified marine-derived Natural Bioactive Compounds As Potential Inhibitors of Oral Cancer. Future Science OA. 2022; 8(3).
[48] Natarajan PM, Umapathy VR. Role of transcriptomics in the study of oral cancer. Frontiers in Oral Health. 2025; 6:1524364.
[49] Natarajan PM, Swamikannu B, Sivaraman NM, Stylin AGSQ. Prevention of Oral Cancer: A Comprehensive Guide. Journal of Pharmacy and Bioallied Sciences. 2024; 16(5): S4239-S4241.
[50] Natarajan PM. Computational Studies on Recent Congeners of Fluoroquinolones and Nitroimidazoles for Their Use in Periodontal Therapy. Journal of Pharmacy and Bioallied Sciences. 2024; 16(5): S4731-S4740.
[51] Natarajan PM, Bhuminathan S, Rajan R, Bindu K, Loganathan K, Veerakumar R. The Crucial Role of Smoking Cessation in Preventing Oral Cancer. Journal of Pharmacy and Bioallied Sciences. 2024; 16(5): S4245-S4247.
[52] Natarajan PM, Bhuminathan S, Leela B, Bindu K, Loganathan K, Ramachandran V. Smoking and its Role in Oral Cancer. Journal of Pharmacy and Bioallied Sciences 16(5): S4242-S4244.
[53] Vidhyarekha U, Natarajan PM, Bhuminathan S, Sabarinathan J, Suba R, Vijayalakshmi P. Role of artificial intelligence in Oral Cancer. Advances in Public Health. 2024. 2024: 3664408.
[54] Ganesan A, Kumar NG, Natarajan PM, Gauthaman J. Automated classification of elongated styloid processes using deep learning models-an artificial intelligence diagnostics. Frontiers in Oral Health. 2025; 5: 1424840.
[55] Umapathy VR, Natarajan PM, Swamikannu B. Regenerative Strategies in Dentistry: Harnessing Stem Cells, Biomaterials and Bioactive Materials for Tissue Repair. Biomolecules. 2025; 15: 546.
[56] Ganesan A, Kumar NG, Natarajan PM. Solanum trilobatum leaf extract-derived silver nanoparticles downregulate the PI3K/AKT/mTOR signaling pathway and attenuate oral squamous cell carcinoma cell proliferation. Journal of Herbmed Pharmacology. 2024; 13(2): 300-307.
[57] Perumal MKK, Renuka RR, Subbiah SK, Natarajan PM. Artificial intelligence-driven clinical decision support systems for early detection and precision therapy in oral cancer: a mini review. Frontiers in Oral Health. 2025; 6: 1592428.
[58] Ramesh E, Ganesan A, Lakshmi KC, Natarajan PM. Artificial intelligence-based diagnosis of oral leukoplakia using deep convolutional neural networks Xception and MobileNet-v2. Frontiers in Oral Health. 2025; 6: 1414524.

[59] Ganesan A, Kumar NG, Natarajan PM. Anticancer activity of silver nanoparticles synthesized from aqueous leaf extract of Solanum trilobatum (Purple fruit pea eggplant) on human oral cancer cells. Journal of Herbmed Pharmacololgy. 2024; 13(2): 260-268.
[60] Palanisamy CP, poompradub S, Sansanaphongpricha K, Subramani K, Sonsudin F. Increased expression levels of PDGF and VEGF magnify the wound healing potential facilitated by biogenic synthesis of silver nanoparticles. Nano-Structures & Nano-Objects. 2024; 39: 101236.
[61] Pei J, Palanisamy CP, Jayaraman S, Natarajan PM, Umapathy VR, Roy JR, Thalamati D, Ahalliya RM, Kanniappan GV, Mironescu M. Proteomics Profiling of Extracellular Vesicle for Identification of Potential Biomarkers in Alzheimer's Disease: A Comprehensive Review. Ageing Research Reviews. 2024; 99: 102359.
[62] Xi J, Wang T, Xian P, Liu X, Du M, Yang H, Palanisamy CP, Lin W, Long Q. Proteomic insights uncover enhanced neurotherapeutic potential in conditioned mesenchymal stem cell-derived extracellular vesicles. Extracellular Vesicle. 2024; 3: 100037.
[63] Pei J, Natarajan PM, Umapathy VR, Swamikannu B, Sivaraman NM, Krishnasamy L, Palanisamy CP. Advancements in the synthesis and functionalization of zinc oxide-based nanomaterials for enhanced oral cancer therapy. Molecules. 2024; 29(11): 2706.
[64] Gatasheh MK, Natarajan SR, Krishnamoorthy R, Alsulami TS, Rajagopal P, Palanisamy CP, Veeraraghavan VP, Jayaraman S. Molecular analysis to identify novel potential biomarkers as drug targets in colorectal cancer therapy: an integrated bioinformatics analysis. Molecular and Cellular Oncology. 2024; 11(1): 2326699.
[65] Pei J, Yan Y, Jayaraman S, Rajagopal P, Natarajan PM, Umapathy VR, Gopathy S, Roy JR, Sadagopan CS, Thalamati D, Palanisamy CP, Mironescu M. A review on advancements in the application of starch-based nanomaterials in biomedicine: Precision drug delivery and cancer therapy. International Journal of Biological Macromolecules. 2024; 130746.
[66] Pei JJ, Yan Y, Palanisamy CP, Jayaraman S, Natarajan PM, Umapathy VR, Gopathy S, Roy JR, Sadagopan JC, Thalamati D, Mironescu M. Materials-based drug delivery approaches: Recent advances and future perspectives. Green Processing and Synthesis. 2024; 13: 20230094.
[67] Pei JJ, Deng W, Liu Y, Guo Y, Chen J, Abdu H, Khan MR, Palanisamy CP, El-Aty AM. A Comprehensive Review of Cornus officinalis: Health Benefits, Phytochemistry, and Pharmacological Effects for Functional Drug and Food Development. Frontiers in Nutrition. 2023; 10: 1309963.
[68] Alugoju P, Palanisamy CP, Anthikapalli NVA, Jayaraman S, Prasanskulab A, Chuchawankul S, Dyavaiah M, Tencomnao T. Exploring the anti-aging potential of natural products and plant extracts in budding yeast Saccharomyces cerevisiae: A review. F1000Research. 2023; 12: 1265.
[69] Lavanya M, Krishnamoorthy R, Alshuniaber MA, Manoharadas S, Palanisamy CP, Veeraraghavan VP, Jayaraman S, Rajagopal P, Padmini R. Formulation, characterization and evaluation of gelatin-syringic acid/zinc oxide nanocomposite for its effective anticancer, antioxidant and anti-inflammatory activities. Journal of King Saud University-Science. 2023; 35: 102909.
[70] Palanisamy CP, Poompradub S, Sansanaphongpricha K, Jayaraman S, Subramani K, Sonsudin F. Biosynthesis of silver nanoparticles (AgNPs) using ethanolic extract of Nigella sativa (L.) seeds promotes wound healing via PDGF and VEGF signalling pathways activation. Biocatalysis and Agricultural Biotechnology. 2023; 54: 102970.
[71] Prasad M, Jayaraman S, Natarajan SR, Veeraraghavan VP, Krishnamoorthy R, Gatasheh MK, Palanisamy CP, Elrobh M. Piperine modulates IR/Akt/GLUT4 pathways to mitigate insulin resistance: Evidence from animal and computational studies. International Journal of Biological Macromolecules. 2023; 253: 127242.